UNDERWATER TARGET DETECTION WITH HYPERSPECTRAL REMOTE-SENSING IMAGERY

Sylvain Jay, Mireille Guillaume

Institut Fresnel - Domaine Universitaire de Saint-Jerome
Avenue Escadrille Normandie-Niemen
13397 Marseille Cedex 20

1. INTRODUCTION

In hyperspectral supervised target detection, one of the most widely used filters is the MF ([1]):

$$y = D_{MF}(\mathbf{x}) = (\mu_{0,t} - \mu_{0,b})^t \Gamma^{-1} \mathbf{x} \tag{1}$$

In the case of underwater target, the measured spectrum is considerably distorted by the water column. So, it would be interesting to insert a bathymetric model in the expression of the MF, in order to correct these spectral distortions.

Firstly, we will present the bathymetric model of reflectance, to insert it in the filter expression. Then, we will compare this new filter with classical filters and we will study the influence of estimation errors on model parameters, on detection.

2. BATHYMETRIC MODEL OF REFLECTANCE

Various models have been developed to build subsurface reflectance from bottom reflectance and water constituents. The most common has been proposed by Maritorena et al. [2]:

$$r_{rs}(\lambda) = r_{rs,\infty}(\lambda)(1 - e^{-2k(\lambda)H}) + \frac{r_B(\lambda)}{\pi} e^{-2k(\lambda)H} \tag{2}$$

where $r_{rs,\infty}(\lambda)$ represents the subsurface remote-sensing reflectance over an optically deep water column, $r_B(\lambda)$ the bottom albedo, $k(\lambda)$ the attenuation coefficient and H the depth.

$r_{rs,\infty}(\lambda)$ and $k(\lambda)$ depend on the water quality through absorption and backscattering coefficients, and therefore, through three main optically active constituents: phytoplankton pigments, gelbstoff (or CDOM) and non algal particles. In [3], Brando et al. express these coefficients as the sum of their contributions as

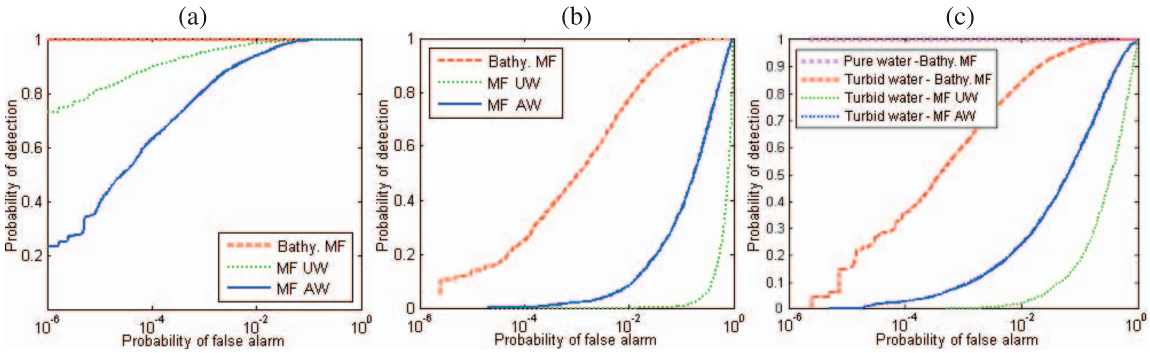

Fig. 1. *ROC curves for simulated data (target=galvanized metal): a) Pure water (H=2m), b) Pure water (H=50m), c) Pure and turbid water (H=11m).*

following:

$$a(\lambda) = a_w(\lambda) + C_\varphi a^*_\varphi(\lambda) + C_{CDOM} e^{-S_{CDOM}(\lambda-\lambda_0)} + C_{PNA} a^*_{PNA}(\lambda_0) e^{-S_{PNA}(\lambda-\lambda_0)} \quad (3)$$

$$b_b(\lambda) = b_{b,w}(\lambda) + C_\varphi b^*_{b,\varphi}(\lambda_1)\left(\frac{\lambda_1}{\lambda}\right)^{Y_\varphi} + C_{PNA} b^*_{b,PNA}(\lambda_1)\left(\frac{\lambda_1}{\lambda}\right)^{Y_{PNA}} \quad (4)$$

where the index w is related to pure water, φ to phytoplankton, CDOM to gelbstoff and PNA to non algal particles. Reference wavelengths are fixed: $\lambda_0 = 440$nm and $\lambda_1 = 542$nm.
Then, $r_{rs,\infty}(\lambda)$ and $k(\lambda)$ depend only on $a(\lambda)$ and $b_b(\lambda)$ ([4],[5]).

3. DEVELOPMENT OF THE BATHYMETRIC MATCHED FILTER

The eq. 2 can be written in the following matrix form for every wavelength in the VIS/NIR range:

$$\rho = \mathbf{K}\rho_0 \quad (5)$$

where $\rho = \mathbf{r}_{rs} - \mathbf{r}_{rs,\infty}$, $\rho_0 = \frac{1}{\pi}\mathbf{r}_B - \mathbf{r}_{rs,\infty}$, $\mathbf{K} = diag(e^{-2k(\lambda_1)H}, ..., e^{-2k(\lambda_L)H})$ and L is the number of wavelenghts. We consider the spectral vector ρ as a gaussian random vector with mean $\mu \triangleq E(\rho)$ and covariance matrix $\Gamma \triangleq E\left[(\rho-\mu)(\rho-\mu)^t\right]$.
Then, assuming the background and the target have the same covariance matrix, we can develop the LRT (Likelihood Ratio Test) to obtain the final expression of the bathymetric matched filter (the index t means target, and b means bottom).

$$y = D_{bathy}(\rho) = (\mathbf{K}^{-1}\rho)^t \Gamma_0^{-1}(\mu_{0,t} - \mu_{0,b}) \quad (6)$$

4. RESULTS

4.1. Known parameters

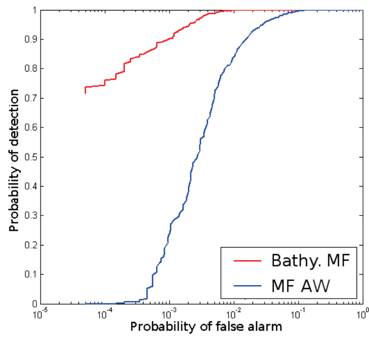

Fig. 2. ROC curve for real data (H=0.32m)

Our algorithm has been tested on both simulated and real data. The wavelength range is fixed at 400-700nm. The bottom is built from a random linear mixture of quartz, feldspar and mica, whereas target spectra are chosen from the USGS spectral library. Once attenuated by the water column, a white noise (σ=0.02) is added to model the sensor noise.
We compare the bathymetric filter with two versions of the classical MF given by eq. 1. The first version called MF UW, is obtained estimating the covariance matrix with the bottom data ρ_0, whereas the second one called MF AW is implemented estimating the covariance matrix with the subsurface data ρ. Results are shown in Fig. 1: in pure water, bathymetric MF can detect up to 50m with a probability of detection (PD) of 0.5 for a probability of false alarm (PFA) of 10^{-3}. For very turbid waters, it also overcomes classical filters detecting galvanized metal over 11m.
ROC curve in Fig. 2 is obtained from real data (H=0.32m), considering the employed port water as pure water (for such shallow areas, the attenuation is mainly caused by pure water). Therefore, we can confirm the performances presented previously in the simulations.

4.2. Influence of parameters estimation errors on detection abilities

Some parameters of the eq. 6 can be unknown: usually, mean μ and covariance matrix Γ are estimated with their ML estimates ([1]). The coefficients $a(\lambda)$ and $b_b(\lambda)$ are supposed to be constant in the whole area so they can be measured once. But, it would be interesting to estimate depth, which is more difficult to measure everywhere in the scene. For shallow waters, the ML estimate is very precise, no matter how the water is. For deeper waters, the influence of concentrations is greater, and the estimation error on H can be studied against the estimation errors on the three concentrations (see Fig. 3). The estimation of H is not highly sensitive against C_φ and C_{PNA}, but

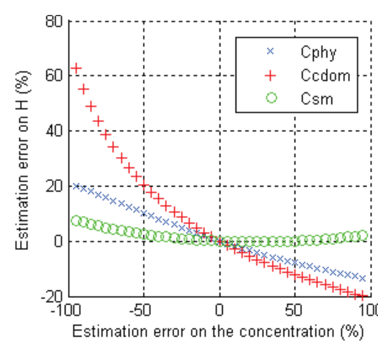

Fig. 3. Estimation error on depth against estimation error on C_φ, C_{CDOM} and C_{PNA} (H=10m)

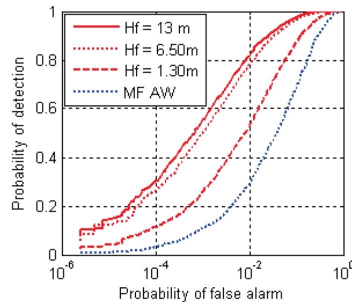

Fig. 4. ROC curves plotted with different erroneous values of H_f in the filter. True depth is 13m.

a relatively precise estimation of C_{CDOM} is needed to keep a good estimation of H and therefore, a good detection rate. Indeed, with a 50$\%$ error on the estimation of H, the PD is reduced of 0.07 for a PFA of 10^{-3}, whereas it's reduced of 0.3 with a 90$\%$ error (see Fig. 4).

5. CONCLUSION

We developed a new version of the MF which outperforms classical MF for underwater target detection. In simulations, bathymetric MF detects the studied target up to 50m in pure water, and up to 11m in turbid water. It also turns out that it works better on real data. If H is unknown, it can be ML-estimated, and a 50$\%$ error does not affect much the detection performances. In future works, we will also estimate the concentrations, to obtain an autonomous system for underwater target detection.

6. REFERENCES

[1] D. Manolakis et G. Shaw, "Detection algorithms for hyperspectral imaging applications," *IEEE Signal Processing Magazine*, pp. 29–43, 2002.

[2] B. Gentili S. Maritorena, A. Morel, "Diffuse reflectance of oceanic shallow waters - influence of water depth and bottom albedo," *Limnology and Oceanography*, vol. 39, pp. 1689–1703, 1994.

[3] V.E. Brando et al., "A physics based retrieval and quality assessment of bathymetry from suboptimal hyperspectral data," *Remote Sensing of Environment*, , no. 113, pp. 755–770, 2009.

[4] M. Velez-Reyes et W. Rivera C. Gerardino-Neira, J. Goodman, "Sensitivity analysis of a hyperspectral inversion model for remote sensing of shallow coastal ecosystems," *IEEE International Geoscience and Remote Sensing Symposium*, 2008.

[5] C.J Legleiter et D.A Roberts, "A forward image model for passive optical remote sensing of river bathymetry," *Remote Sensing of Environment*, , no. 113, pp. 1025–1045, 2009.